Recycling construction and industrial landfill waste material for backfill in horizontal ground heat exchanger systems

Yasameen Al-Ameen *,a, Anton Ianakiev [a], Robert Evans [a]

[a] School of Architecture, Design and the Built Environment, Nottingham Trent University, Nottingham, UK

Abstract

This research experimentally and numerically investigates the possibility of recycling some low cost construction and industrial waste landfills materials as potential backfills in horizontal ground heat exchangers (HGHE). The aim of this study was to compare the temperature distribution development in different backfill materials with respect to time. The tested materials include sand, crushed basalt, broken brick, crushed concrete, and metallic by-products including copper slag, aluminium slag, mill-scale and iron ores (fine and pellets). Initial thermal testing on these materials in an environmental climatic chamber indicated concrete and crushed brick had similar performance to sand, whereas metallic materials had better performance by up to 77% improvement compared to sand. Various percentages of the backfill material (20, 40, 60, 80 and 100%) blended with the remaining percentage of sand showed that the higher the percentage addition of the waste material, the better the heat storage of the enhanced sand. Particle size distribution was also a significant parameter in backfill selection, where medium sized particle sizes (1.18-2 mm) performed 92% better compared to course and fine gradations of the same material. An experimental set-up of a HGHE system was then constructed and filled with the best performing backfill materials to determine the heat storage and release processes on the thermal performance of the system. The paper also reports results from a transient three-dimensional finite volume model developed in ANSYS Fluent 17.2 computational fluid dynamic (CFD) software of a thin section of a HGHE. The experimental and numerical model were used to predict and analyse the temperature distribution developing within the surrounding backfill material with respect to charging (heating) and discharging (extracting heat) modes of the HGHE. Results obtained from both experimental and numerical studies show the temperature range and duration of hot water produced from the system were in line with low temperature space -heating guidelines and that mill-scale, copper slag and aluminium slag were the best backfill materials, where the thermal capacity of the HGHE system can be doubled using these materials, compared to the use of sand alone. Congruence between the numerical simulations and experimental data was found.

Keywords: (Energy, Horizontal ground heat exchanger, Waste materials, Temperature distribution, Space heating)

1. Introduction

1.1. Background

Growing environmental concerns including climate change, air pollution and depletion of natural fossil resources require urgent long term sustainable development actions (Dincer and Rosen, 2004; Ozyurt and Ekinci, 2011; Diaz, Sierra and Herrera, 2013). Energy supply, and associated energy prices, are gradually becoming more sustainable by introducing renewable energy resources, particularly solar, wind, hydropower and geothermal energy (Bourrelle, Andresen and Gustavsen, 2013; Esen and Yuksel, 2013; Lund *et al.*, 2016). Recent developments into incorporating these resources to provide heating and cooling demands of buildings is becoming more popular in the developing world. Solar photovoltaic and thermal collector technologies have been proven to provide sustainable electricity and heat to homes, however, the mismatch between the time the energy is available (sunlight hours) and the time it is required (demand period) has led to further developments in thermal energy (heat) storage systems (Ozgener and

Hepbasli, 2005; Henning, 2007; Axaopoulos and Fylladitakis, 2013; Esen and Yuksel, 2013; Gao *et al.*, 2013; Emmi *et al.*, 2015; Awani *et al.*, 2017).

For low temperature space heating purposes, the ground can be used as an efficient, clean, cheap, low maintenance and sustainable heat storage (Esen and Yuksel, 2013). Ground heat exchangers (GHE) are outstanding heating systems and have been used for a number of years in the USA, Europe, Turkey, and Japan (Florides and Kalogirou, 2007; Tarnawski *et al.*, 2009; Esen and Yuksel, 2013; Sarbu and Sebarchievici, 2014; Dehghan B., 2017; Stylianou *et al.*, 2017). Shallow horizontal forms of ground heat exchangers (HGHE) offer lower complexity and economic advantages compared to vertical designs and, although more land area may be required to meet a given heat exchange requirement, they continue to be an appealing technology for residential and smaller non-residential applications with a low temperature requirements of 35 to 70℃ (Wong B., Snijders A., 2006; Chiasson, 2010; Garcia Gonzalez *et al.*, 2012; Simms, Haslam and Craig, 2014; Go *et al.*, 2015; Kupiec, Larwa and Gwadera, 2015; Yoon, Lee and Go, 2015; Rees, 2016; Wei *et al.*, 2017). A HTF (heat transfer fluid) is circulated through buried heat exchanging pipes to extract the stored heat from the soil storage upon requirement. The buried pipes are surrounded by soil, and hence the performance of the HGHEs is highly dependent on ground heat-transfer characteristics (Ball, Fischer and Hodgett, 1983; Esen, 2000; Qoaider, Kiwan and Thabit, 2016).

Various studies and reviews have been conducted on the design, testing, optimisation, and simulation of GHEs although most researchers focused on monitoring GHEs coupled with ground source heat pumps (GSHP) to maintain steady and comfortable indoor temperatures (Ball, Fischer and Hodgett, 1983; Leong, Tarnawski and Aittomäki, 1998; Hepbasli, Akdemir and Hancioglu, 2003; İnallı and Esen, 2004; Florides and Kalogirou, 2007; Gan, Riffat and Chong, 2007; Cui, Yang and Fang, 2008; Koyun, Demir and Torun, 2009; Esen, Inalli and Esen, 2009; Wu *et al.*, 2010; Garcia Gonzalez *et al.*, 2012; Garber, Choudhary and Soga, 2013; Sarbu and Sebarchievici, 2014; Sivasakthivel, Murugesan and Thomas, 2014; Bertermann, Klug and Morper-busch, 2015; Naylor, Ellett and Gustin, 2015; Esen and Turgut, 2015; Kim *et al.*, 2016a, 2016b; Luo *et al.*, 2016; Esen, Esen and Ozsolak, 2016; Stylianou *et al.*, 2017; Wei *et al.*, 2017). Although there is a need to be able to calculate HGHE performance, there has been less progress in developing validated models, and consequently design methods remain relatively simplified with design data tables and charts often being used in practice (Rees, 2016). Experimental work on HGHEs has included Esen and Yuksel (2013) investigating heating a greenhouse in Turkey's climate conditions using biogas, solar and ground energy and concluding that the ground can be successfully used for greenhouse heating purposes. Inalli and Esen (2004) also experimentally investigated a HGHEs connected to a GSHP to confirm the effects of the parameters including the mass flow rate of the HTF, the buried depth of soil, the coupled heat exchanger, and sewer water on the performance of the system to be used for space heating applications. Kim *et al.* (2016b) experimentally and numerically investigated the performance of a HGHE simulated steel box filled with dried Joomunjin sand, comparing coil and slinky heat exchange pipes performance in HGHEs, and concluded slinky-type was better and that GHEs type and soil thermal conductivity are the main factors determining the heat exchange rate of a GHE, whereas the pipe diameter did not have any effect on the GHE performance. Wu *et al.* (2010, 2011) studied the thermal performance of a HGHEs ground-coupled GSHP in a UK climate both experimentally and numerically and concluded that heat extraction from the HGHEs increased with ambient temperature and soil thermal conductivity, however it decreased with increasing HTF temperature. Congedo *et al.* (2012) carried out computer simulations on several HGHEs configurations considering soil thermal conductivity, installation depth, and fluid velocity and concluded that the optimal soil type to use around the heat exchanging pipes was that with the highest thermal conductivity.

Recent research into solar assisted HGHE systems has mostly been devoted to optimising and improving the performance of systems by the addition of GSHP's, with much less focus on the backfill media used for storage and the air temperature fluctuations caused by the proximity of HGHEs to the ground surface (Hepbasli, Akdemir and Hancioglu, 2003; Li *et al.*, 2006; Hu *et al.*, 2013; Shang, Dong and Li, 2014). Careful attention has to be paid to the use of backfilling materials and installation procedures to ensure there is good contact between the pipe and the ground in the finished heat exchanger (Rees, 2016). There is an increased awareness that landfills are overfilling and that recycling waste is important (Lund, 2010; Esen and Yuksel, 2013). The UK waste statistics regulation published data showing that 148 million tonnes of waste was produced in 2014 from combined commercial & industrial (C&I) and construction, demolition and excavation (CD&E) sectors (DEFRA, 2017). CD&E landfills receive construction and demolition debris, which consists of road material including crushed concrete and brick, some metals, excavated material, demolition waste, construction/renovation waste and, site clearance waste (Deloitte, 2015). C&I landfills receive industrial and commercial solid wastes, or generator wastes (Deloitte, 2015). Reducing and recycling these materials conserves landfill space, reduces the environmental impact of producing new materials, creates jobs, and can reduce overall project expenses through avoided purchase/disposal costs (WRAP, 2010).

1.2   Study Objectives

The temperature propagation and distributions in HGHE systems are important when designing storage equipment to simulate working capacity and thermal performance. The aim of this research was to experimentally and numerically investigate the temperature distributions of an insulated HGHE system using various ~~low cost~~low-cost CD&E and C&I recycled waste materials as potential backfill materials to form a comparison study. The tested materials include sand, crushed basalt, broken brick, crushed concrete, and metallic by-products including copper slag, aluminium slag, mill-scale and iron ores (fine and pellets). After initial material thermal testing, an experimental set-up of a small scale HGHE was tested in the laboratory and a 3D computational fluid dynamic (CFD) numerical model was developed in ANSYS Fluent 17.2 to assess the heat transfer in each of the backfill materials for charging (heating) and discharging (extracting heat). Testing and comparing various backfill materials under the same working conditions (including the same solar radiation, ambient air temperature, collector materials, insulating materials and HGHE dimensions) means a comparative analysis can be made between experimental and numerical results to validate them. These points will assist designers in designing HGHEs.

2   Materials and Methods

2.1   Experimental Set-up

An experimental system was previously designed and built at Nottingham Trent University to investigate and evaluate the thermal performance of a small scale underground horizontal ground heat exchanger system in heating mode (charging) and extracting mode (discharging) designed for a 1 kW heating load at design conditions. A schematic diagram of the system is shown in Fig. 1~~Figure 1~~. Table 1~~Table 1~~ summarises the main technical information on the different soil backfill media as well as varying outlet mass flowrate were studied from the storage as mentioned in Al-Ameen *et al.* (2017).

Fig. 2~~Figure 2~~ shows a schematic diagram of the experimental storage box set-up used in the HGHE system, the same geometry is used in the developed numerical model. The outer dimensions of the model were 1.15 m x 0.65 m x 0.125 m, this provided insulation and containment to the backfill material used within the storage; the internal dimensions of the backfill material volume were 1 m x 0.5 m x 0.125 m. A network of 10 mm diameter copper pipes with a wall thickness of 1.5 mm, run in a curved configuration as illustrated in Fig. 2. The total length of buried pipe in the HGHE was 5 m and contains the heat transfer fluid (water). The height of the buried pipe is 62.5mm from the top and bottom of the storage pit (middle centreline) and has horizontal spacing distances between the straight sections of 85 mm. The heating cables were used to heat the surrounding backfill material in the HGHE to reach temperatures of 65℃ ±5℃, simulating temperatures achieved from solar thermal collectors, and then cold water was circulated in the system to extract the thermal energy stored in the backfill material. These pipes were connected to a cold-water storage tank and the system relied on gravity, rather a ground source heat pump to operate it. A schematic of the complete system is illustrated in Fig. 1~~Figure 1~~. The thermo-physical properties of materials utilized within HGHE storage are illustrated **Reference source not found.**~~Table 2.~~ .

2.2   Measurements

Temperature and flowrate measurements were monitored and recorded during the testing phase. These are discussed in the subsequent sections.

2.2.1   Temperature

To measure the temperature of the backfill material and the circulating HTF in the experimental HGHEs, a series of K-type thermocouples were installed. Several considerations were considered when selecting the K-type thermocouples in terms of influencing measured results. K-type thermocouple sensors provide the widest operating temperature range and generally work in most applications because they are nickel based and have good corrosion resistance. However, they are prone to stress, strain making them brittle and corrode, particularly as they age. K-type thermocouples are stable for short periods at certain temperatures, after which they tend to drift in a positive direction. The size of the drift is dependent on the temperature and usually occurs at temperatures above 760 °C. Also, prolonged exposure to high temperatures (above 427 °C) makes the thermocouples age faster and in reduced oxygen environments "green rot"

occurs which oxidizes the thermocouple. The k-type thermocouples were used in the experiment to take measurements between 10-75 °C and therefore were not prone or exposed to affects from aging, stress/strain at high temperatures and drifts in temperature readings. Therefore, the results from thermocouples can be made accurately. For the exposed K-type thermocouples, the tolerance is given as ± 1.5K between -40 and 375 °C. The total uncertainties of the temperature's measured at various location are listed in Table 5.

Forty thermocouples were used to measure the temperature of backfill material, these were placed at ten locations in plan view as illustrated in Fig. 2Figure 2 and repeated on four layers: at the centre layer (0 m) and at distances 0.02 m, 0.04 m and 0.06 m from the centre layer. Two further thermocouples were used to measure the temperature of the HTF at the inlet and outlet of the HGHE. The average inlet temperature of the HTF was 15-18℃. The density, thermal conductivity, specific heat and kinematic viscosity of the HTF used in the numerical model were determined according to this temperature range. The ambient and room temperatures were also measured using thermocouples and thermometers.

2.2.2   Flowrate

The heat transfer between the backfill material and the HTF was affected by the operating flowrate of the system. The flowrate of the circulating HTF in the closed loop HGHE was measured using a flowrate meter and controlled using mechanical valves fitted at various locations in the system as illustrated in Fig. 1Figure 1. The average HTF volume flowrate ranged between 0.1 to 0.7 L/min (or mass flowrate $\dot{m}_{HTF}$ is between 0.0017 to 0.012 kg/s) and the corresponding velocities were calculated using Eq. 1, equation 1 to be between 0.04 to 0.30 m/s. These calculated values were utilised in the numerical study and were dependant on experimental results. The Reynolds number was calculated to be between 280 to 2100 using Eq. 2 equation 2 for the range of flows used during testing, indicating the flow was laminar in all cases. The convection heat transfer coefficient (h_c) was taken as the upper limit between the free and forced convection coefficients and was calculated using Eq. 3-6 equations 3-6 to be between 13 to 35 W/m²K for the h_c in the bottom and top of the HGHE section layer.

$$\overrightarrow{V_{HTF}} = \frac{\dot{m}_{HTF}}{\rho_{HTF}\, A_{pipe}} \qquad (1)$$

$$Re_x = \frac{\rho_{HTF}\, V_{HTF}\, D_H}{\mu} \qquad (2)$$

$$Pr = \frac{\mu C p_{HTF}}{k_{HTF}} \qquad (3)$$

$$Nu = 0.664\, Re_x^{1/2}\, Pr^{1/3} \qquad (4)$$

$$Pe = Re_x Pr \qquad (5)$$

$$h_c = \frac{Nu\, k_{HTF}}{D_H} \qquad (6)$$

Where: V_{HTF} is the mean velocity of the HTF (m/s), $\dot{m}_{HTF}$ is the mass flowrate of the HTF (kg/s), ρ_{HTF} is the density of the HTF (kg/m³), A_{pipe} is the cross-sectional area of the pipe (m²), Re is the calculated Reynolds number for the flow in the pipe, Q is the volumetric flowrate (m³/s), D_H is the hydraulic diameter of the pipe (m), h_c is the convection heat transfer coefficient (W/m²K), Nu is the Nusselt number, k_{air} is the thermal conductivity of air (W/mK), L is the distance from the pipe to the location of the top/bottom surface plane (m), Pr is the Prandtl number, U_∞ is the free stream velocity (m/s), v is the kinematic viscosity of the HTF (m²/s), μ is the dynamic viscosity of the HTF (Ns/m²), Cp_{HTF} is the specific heat of the HTF (J/kgK) and k_{HTF} is the thermal conductivity of the HTF (W/mK).

2.3   Materials

Twelve materials were utilised as backfill media's in the HGHE for both experimental testing and the developed numerical model. These were Leighton buzzard sand (LB), two types of crushed brick (TBW, TBR), Iron (pellets IP and two filling types IFN, IFO), Aluminium slag (AO), Copper slag (CS), Mill-scale (MS), Basalt rock (crushed fine BAF and course BAC) and crushed concrete (CON) as illustrated in Fig. 3Figure 3. From a designer's point of view,

these selected materials are widely available and are waste produced from construction and industrial processes (Deloitte, 2015). Waste material would typically go to landfill, increasing the burden on landfill loading and operation, and subject to landfill tax in the UK. In the UK, waste management plans (WMP) have been developed by each of the government bodies within England, Wales, Scotland and Northern Ireland that are responsible for waste management strategies and waste prevention plans (Deloitte, 2015). Government programmes have encouraged the setting of targets for recycled content for construction products, which in turn led to demand for high-recycled content (Deloitte, 2015). The waste materials that are still usable are donated to non-profit organizations to be recycled and reused in different applications (WRAP, 2010; Deloitte, 2015). This keeps the material out of the landfill and means the material is being sustainably taken advantage of at a low cost (WRAP, 2010).

Each of the materials were prepared for use prior to testing. The materials were placed in an oven at 105 °C to remove moisture. All the material were then sieved to remove fine particles passing a 0.16 mm sieve. In this study, the material's thermophysical properties determine their heat storage capacity. **Error! Reference source not found.**Table 2 material's properties including particle size, gradation classification, bulk and particle density, ,porosity, thermal conductivity and specific heat capacity. Material testing was conducted according to British Standard testing procedures for granular materials (BS 5930:1981, BS 1377, BS 7591-2:1992, BS EN 12667:2001). Most of the waste materials have a higher density and better thermal properties than sand alone, which can improve the overall thermal capacity of a HGHE system and improve the heat exchange efficiency between the backfill medium and the tube containing the HTF. Additional preparation was conducted on some of the materials whereby the materials were further sieved into individual sizes of between <0.6 mm, 0.6-1.18 mm, 1.18-2 mm to investigate the influence of grain size on heat storage.

3   *Thermal testing of materials*

The proposed backfill materials were tested in an environmental climatic chamber (Model: FDM C-SERIES). This was achieved by filling 10 litre containers with each of the backfill materials and placing RS Pro K-type thermocouples (chromel-alumel) to measure temperature at various locations in the containers. The environmental chamber was set for heating (up to 70 ℃) and cooling cycle to simulate heat storage. Once the material in the containers had reached a homogenous temperature of 70±2 ℃, they were left to cool to ambient room temperature (≈ 20 ℃). Thermocouple sensors were attached to a central data logger to monitor temperature. Temperature readings were recorded at 5-minute intervals internally for the environmental chamber (T_{EC}), externally for the room temperature (T_{room}) and at five locations in the container as illustrated in Fig.4 to measure the temperature of the material at different positions in response to the heating and cooling pattern. The T_{midd} was plotted against time for the different proposed backfill materials as illustrated in Fig. 7 – 9. Temperature readings were recorded at 5-minute intervals internally for the environmental chamber (T_{EC}), externally for the room temperature (T_{room}) and at three locations in the container. Tests were also conducted with a sand (LB) filled control container and repeated three times, for comparison. The results are discussed in section 6-1.

4   *Modelling approach*

It is important to understand how to improve the thermal performance of the insulated HGHE using different backfill materials. Therefore, a reliable mathematical model of the HGHE model is essential in completing the task. Testing and validation of the experimental model is essential to ensure the accuracy and validity of the HGHEs simulation. This study is concerned with validation of a thin section of HGHE storage model using different backfill materials to compare the temperature distributions. The temperature distributions in the HGHE sections were conducted using a computational fluid dynamic software (CFD). CFD analysis obtains qualitative and quantative information about fluid flow and heat transfer performance of systems. The HGHE system can be modelled as a three-dimensional transient heat conduction temperature field problem. The model was set-up with: (a) internal heat generation in the HTF to simulate storing thermal energy to the backfill medium (HGHE charging) and; (b) internal heat generation in the backfill medium to extract stored thermal energy from the backfill material (HGHE discharging). The assumptions in this model are that the heat transfer occurs by conduction and that convection and radiation effects are insignificant,. Heat conduction is the dominant type of heat transfer in soils and granular materials. Heat convection occurs in granular material depending on the moisture content within the material. The materials used in this research were all used on a dry basis and therefore, it is reasonable to assume that due to no moisture, heat transfer affects from convection are negligible. Furthermore, radiation usually makes a negligible contribution to heat transfer at normal atmospheric temperature. The total contribution of radiation to the heat transfer process is estimated to be less than

1% in sands and much less in finer-grained soils (Farouki, 1986; Rees *et al.*, 2000; Deru, 2003). Additional subsequent assumptions in the analysis have been made including:

(1) A closed system is in operation
(2) The thermophysical properties of the backfill material are uniform (**Error! Reference source not found.**Table considered as a single volume
(3) The heat transfer in the backfill material is considered to be symmetrical
(4) The backfill material is assumed to have no moisture content
(5) The copper tube wall thickness (1.5 mm) was very small and therefore pipe conduction resistance is neglected
(6) The top and bottom wall surfaces of the HGHE were considered to be 293 K at the start of each simulation
(7) The starting temperature of the inlet HTF was also assumed to be 293 K

4.1   Developed model

CFD simulations were performed within ANSYS FLUENT, version 17.2. Meshing, set-up and the solution were conducted in workbench. The geometry was constructed in solid works and imported as STEP format into the design modeller part of ANSYS. The five parts of the geometry, velocity inlet, pressure outlet and external shell wall were specified as illustrated in Fig. 5. ANSYS workbench automatically generated a mesh for the model. However, a finer mesh was incorporated around the HTF and surrounding copper tube (element size 0.0005m), where the temperature gradient is the steepest and a course mesh was incorporated for the soil, insulation and cover layers (element size of 0.01 m). These values were obtained from undertaking a grid independence study on the mesh to report accurate CFD simulation results. The mesh grid independence evaluation was conducted by starting with a default mesh and assessing the results, the element size was then gradually reduced, and the error was quantified. This process was repeated until the error was within an acceptable tolerance level. Fig. 6 shows results from the mesh independence evaluation as a graph of number of elements (millions) against the average temperature at the outlet for a run on the charging of the LB backfilled storage (at 8 hours). Fig. 6 indicated that a solution value was reached with 8 million elements (6 million nodes) that is independent of the mesh resolution which can be used for further analysis. In terms of the numerical model used in this study, the 3D mesh consisted of mixed tetrahedron and hexahedron elements as illustrated in Fig. 7. This mesh was utilized to give results within the acceptable error tolerance level as illustrated from the accuracy of output temperature shown in Fig. 7. The mesh was then exported to the fluent software where the governing equations were set, and the material properties and cell zone conditions where defined.

The boundary conditions were then placed. The finite volume mathematical model (FVM) relies on the laws of thermodynamics for heat transfer and conservation of mass and energy, and utilizes continuity partial differential equations. A laminar model flowrate was used in the heat exchanger pipe. A velocity inlet of 0.3 m/s, obtained from previous experimental testing, was set. A pressure outlet with a zero backflow and convection was placed at the wall boundaries. Thermal conditions are also satisfied for heating and cooling modes of the storage. The boundary conditions conditions specified in both the charging and discharging models are summarised in Table 2. Thermophysical properties of materials used in this study

Material and Abbreviation	Particle Size (mm)	Thickness (m)/ Gradation Classification	ρ_b (kg/m³)	ρ_s (kg/m³)	ϕ (%)	k (W/mK)	Cp (J/kg K)
HGHE construction materials:							
Cover (MDF)	-	0.025m	700	-	-	0.15	1700
Insulation (XEPS)	-	0.05m	33	-	-	0.03	1131
Copper Pipe	-	0.003m	8950	-	-	401	385
Water liquid (HTF)	-		1000	-	-	0.60	4200
Air (external environment)	-		1.23	-	-	0.02	1006
HGHE backfill materials:							
Leighton Buzzard Sand (LB)	0.16 – 1.18	UG	1562.49	2620.80	40.40	0.38	805.87
Crushed Brick 'W type' (TBW)	0.06 – 5.00	WG	1142.46	2631.37	56.60	0.65	860.02
Crushed Brick 'R type' (TBR)	0.16 – 5.00	WG	974.45	2275.70	57.20	0.62	834.45
Concrete (CON)	0.16 – 14.00	WG	1204.07	2280.30	47.20	1.28	645.33
Basalt rock 'fine' (BAF)	0.16 – 5.00	GG	1496.53	2681.00	44.20	2.04	884.35
Basalt rock 'course' (BAC)	6.30 – 10.00	UG	2389.61	2704.45	49.32	1.24	907.21
Iron ore pellets (IP)	10.00 – 14.00	CG	2080.42	3954.37	47.40	0.56	616.50
Iron Filings 'N type' (IFN)	0.16 – 3.35	WG	2596.82	3728.91	30.38	0.60	580.07
Iron Filings 'O type' (IFO)	0.16 – 3.35	WG	3250.51	3668.17	11.40	0.55	546.14
Millscale (MS)	0.16 – 6.30	UG	2544.48	3133.00	18.80	0.42	652.39
Copper slag (CS)	0.43 – 2.00	UG	1992.03	3399.32	41.40	0.78	557.21

| Aluminium slag (AO) | 0.60 – 2.00 | UG | 1897.96 | 3641.36 | 47.90 | 17.34 | 476.75 |

Table 3Table 3. It is assumed that the top and bottom side of the HGHE are open and the HTF flow runs from the inlet to the outlet through the copper heat exchange pipe. A transient model was assumed, with a time step of 0.001 s.

The results and discussion of the numerical model are given in section 6-2 and 6-3.

5. *Thermodynamic analysis and uncertainty*

A thermodynamic analysis and uncertainty study was conducted to ensure verification and accuracy of data obtained during this study. The thermal performance of the HGHE system was determined by the temperature change in the HTF liquid (difference between inlet and outlet temperatures). According to the first law of thermodynamics, the rate of heat energy transfer into the HGHE equals the rate of heat energy transfer out by the HTF. Eq. 7 Equation 7 was used to calculate the energy required (Q_{in}) to raise the temperature of the backfill in the HGHEs from an initial starting temperature of 293 K to 343 K based on the thermal properties of each of the backfill materials. Table 4, Table 4Table 4 summarises the results obtained for Q_{in} with each of the different tested materials. The heat extracted (Q_{ext}) from the HGHE was also calculated from Eq. 8, using different backfill materials. Cold HTF enters the system at the inlet and passes through the system in the outlet direction to extract the heat stored in the backfill material. The range of Q_{ext} for each material was based on the hot water produced from a low and high flowrate. A high flowrate (HF) of 0.01 kg/s and low flowrate (LF) of 0.0016 kg/s were considered. The Q_{ext} ranged between 5102 kJ (LF) and 1693 kJ (HF) for the backfilled HGHE. Considering the time taken to extract the heated HTF for each flowrate case, the total heat extracted was calculated to be 0.05 kW (LF) and 0.31 kW (HF). The heat exchange rate per pipe length is calculated to be 10 W/m and 62 W/m for LF and HF respectively. This is because at higher flow rates, the HTF passes through the system quickly extracting more heat at a shorter time period. However, due to the faster flow of cold HTF entering the system, the surrounding back-fill cools down at a quicker rate. The system continues to cool down until all the heat is extracted from the HGHEs through the HTF (i.e. back-fill media temperature reduces until it reaches equilibrium with the HTF temperature). In contrast, for lower flow rates, although the HTF flows slowly through the system meaning there is sufficient time for the heat exchange to occur between the backfill and the HTF; the heat is extracted from the system at extremely low rates (in terms of time) for it to be beneficial for hot water heating purposes on the long run.

$$Q_{in} = m_{BF} \cdot C_{p,BF} \cdot (T_{e,BF} - T_{s,BF}) \qquad \text{(eq. 7)}$$

$$Q_{ext} = \dot{m}_{HTF} \cdot C_{p,HTF} \cdot (T_{HTF,o} - T_{HTF,i}) \qquad \text{(eq. 8)}$$

Where: Q_{in} is the energy required to raise the temperature of the backfill material in the HGHE (kJ); m_{BF} is the mass of backfill material in the HGHEs (kg); $C_{p,BF}$ is the specific heat of the backfill material (kJ/kgK); $T_{e,BF}$ is the temperature of backfill material at the end of the heating process (K) ; $T_{s,BF}$ is the temperature of backfill material at the start of the heating process (K) ; Q_{ext} is the energy extracted from the HGHE using the HTF (kJ); $\dot{m}_{HTF}$ is the mass flowrate of the HTF (kg/s); Cp_{HTF} is the specific heat of the HTF (kJ/kgK); $T_{HTF,o}$ is the temperature of the HTF at the outlet of the HGHE system (K) and $T_{HTF,i}$ is the temperature of the HTF entering the HGHE system at the inlet (K).

An uncertainty analysis has also been conducted on the experimental parameters obtained in this study utilizing the accepted method of Holman (1994). Temperatures and mass flow rates were measured experimentally using appropriate instruments as described in section 2.2. The uncertainties of the measured parameters are presented in

Table 5Table 5.

6. *Results and discussion*

6.1 *Thermal testing*

This section is divided into three parts. These are as follows:
- Comparing proposed backfill materials (Section 6.1.1)
- Percentage addition of backfill materials (Section 6.1.2)
- Particle size effect of backfill materials (Section 6.1.3)

6.1.1 *Comparing proposed backfill materials*

Initial thermal testing results comparing all twelve materials are shown as temperature vs. time graphs in Fig. 86Figure 6. Details of thermal testing methodology were mentioned previously in section 3. During testing, the internal temperature of the environmental climatic chamber (EC) was recorded as T_{EC} and the ambient room temperature was recorded as A_{MB}. The point at which the T_{EC} curve starts heating up to 70℃ corresponds to the time the EC was switched on and the material filled containers started the heating cycle. Fig. 86Figure 6 illustrates that it generally took between approximately 14 to 20 hours for the material filled containers to reach a steady homogenous temperature of 70℃ ± 2℃ tolerance. The containers were left in the EC for additional heating until all the temperature curves leveled, then the EC was set for a cooling regime starting at 21.5 hours to cool the containers back down to 20℃. The materials had similar cooling patterns but varied with respect to time. In respect to this work, the time it took the samples to cool to 35℃ was considered as the threshold baseline value from the T_{EC} curve. This value was selected as the baseline because most HGHE systems operate between 35-70℃. Sand (LB) took 6.5 hours to cool down, which was similar to other materials including: TBR, BAC and BAF within ± 0.5 hour. CS and AOO materials however performed 77% better compared to sand, cooling down in 11.5 hours. MS, IFO, IFN also had a relative improvement compared to LB sand by 46%, cooling down in 9.5 hours. TBW on the other hand performed less well and cooled down in 4.5hours, a 30% reduction compared to LB sand. This trend can be explained by the nature of each of the materials. The best performing materials (CS, AOO, MS, IFO, and IFN) are sourced from waste industrial processes of producing copper, aluminium and iron. Their metallic nature means they are better conductors than non-metallic materials due to the close packing nature of the metallic ions in the lattice. In addition, metals usually contain free (delocalised) electrons, which make it easier to transfer heat energy through their solid particles. The amount of energy transferred depends on the mass and specific heat of the materials, where in this case the metallic materials had a higher density and mass compared to the other selected materials. It can be concluded that the majority of the tested materials performed similar or better than LB sand and can therefore be considered to be utilized as alternative to sandy soils in HGHE systems to avoid landfill waste accumulation and encourage recycling of materials.

6.1.2 *Percentage additions of backfill materials*

CS, AOO and MS were further tested to assess:—(I) the effect of blending these materials at different percentages by mass (20, 40, 60, 80 and 100%) to LB sand in order to enhance the properties of LB sand and; (II) the effect of particle size gradation on the retention of heat within the containers. The trend of results for I and II from the three materials (CS, AOO, MS) were similar and therefore only CS was chosen to be presented in the results shown in this paper, for clarity and to avoid repetition. Again, the same thermal testing methodology was used to obtain data in Figure & 10. Fig. 79Figure 7 illustrates the results obtained when blending CS at various percentage (by mass) additions 100%) with the remaining percentage (by mass) of LB sand (i.e. 20 CS indicates 20% CS blended with 80% LB sand). A homogenous mixture was achieved by blending the two counterparts using a dry aggregate mixer. Fig. 79Figure illustrates that LB sand can be successfully enhanced by blending it with CS. Comparing the LB sand alone to when blended with the material shows that there is an increase by 15.4% with 20 CS, 23% with 40 CS, 39% with 60 CS, 54% with 80 CS and 77% with 100 CS. This indicates that as the percentage of CS increases in the container, the thermal contact between the surrounding particles increases and allows more retention of heat. Depending on the required performance of the system, a suitable amount of metallic waste material can be blended with the soil to achieve an improved performance rather than using sand alone.

6.1.3 *Particle size effect of backfill materials*

As illustrated in **Error! Reference source not found.**Table 2, the CS material (as supplied) consisted of particles between 0.43 to 2 mm in size, which was abbreviated to CSA in subsequent figures. CSA was then sieved and sorted into three sizes, these include CSF (<0.6 mm), CSM (0.6-1.18 mm), CSC (1.18-2 mm), the initials after CS denote for all, fine, medium and course gradations respectively. Fig. 108Figure 8 shows the thermal testing results from using particle gradations of CS material. It was found that separating the CS material into different particle sizes could further effectaffect the thermal performance of the material. Fig. 10 i8Figure 8 illustrates that CSA cooled down to an increase of 77% compared to LB sand. CSC and CSM had an overlapping performance, were both containers cooled down (to 35 ℃) in 12 hours, which is an increase of 5.5hours (or 85%) compared to LB sand. The fine gradation, CSF, performed less well compared to CSA, cooling down in 9.5 hours. Similar trends were found in AO and MS materials when tested; where AOM and MSM both achieved an increase of 92% compared to sand alone. Therefore, it can be observed that particle size affects and plays an important role in the thermal performance of the different materials tested. This is because, the porosity, particle size distribution and density of a material has a strong influence on its thermal performance. Porosity is important in granular materials as they make up the void space

8

between the grain particles. These voids create spaces where air can fill up. A film of air around the grains turns the material into a better insulator. The correlation between solid density (γ_s), dry density (γ_d) and porosity (ϕ) is shown in eq. 9. As evident from the results, fine sized particle material cooled down quicker compared to medium and coarse-grained particles. This is because according to eq. 9, a decrease in the particle size or/and an increase in porosity means a decrease in the overall dry density of the material.

$$\gamma_d = \gamma_s (1 - \phi) \qquad\qquad (9)$$

6.2   Numerical modelling

An unsteady transient state simulation was performed on a HGHE model in ANSYS FLUENT v17.2 to assess the transfer of heat for charging and discharging mode and study the thermal performance of the system. The boundary conditions were previously listed in ~~Table 4~~Table 4~~Table 3~~. Re number was calculated to be between 475 to 3353 range of flows used during testing as illustrated in Table 6. The flow was classified to be laminar (Re < 2300) for the three lower flow cases and transitional in the higher flow rate case (2300 < Re < 4000). Transitional flow means there was a mixture of both laminar and turbulent flow in the HGHE, with some turbulence in the centre of the pipe, and laminar flow close to the bends. The Nu number was also theoretically calculated using Eq. 4 and compared to the Nu number obtained from the CFD numerical model for different HTF mass flow rates. The results for Nusselt numbers are tabulated in Table ~~6~~ to form a comparison of results. The theoretical Nu results of 23 to 62 were slightly higher compared to the Nu number obtained from the numerical model of 20 to 59. This shows that results from the numerical model are almost identical for Nu number with a maximum 13~~?~~% variation with respect to theoretical values. Results revealed that Nu numbers almost doubled with respect to flowrate. Also, at low velocities, the Nu numbers indicates that the flow is sluggish, and convection is not very active. However, increasing the HTF velocity in the pipe, in turn increases the Re in the streamwise direction which had favourable results on the Nu number enhancing the heat transfer. The convection heat transfer coefficient (h_c) was also calculated using Eq. 6 to be between 2 to 6 kW/m²K as illustrated in Table 6.

Several backfill materials were tested and simulated in the HGHE section both numerically and experimentally, however, in this paper only the results from CS, which achieved the best performance and LB sand, which is a standard soil used for comparison are discussed. The fluent program was initialized using hybrid initialization and run by iteration command. The coupled solver was used and a time step size was specified of 0.001s. Temperature distributions are shown in Fig.~~Figures~~ 9~~11~~ ~~12~~ 14 for charging and discharging of the HGHE after 8 hours (where Figure ~~Fig. Figures~~ 9~~11~~ ~~&11~~
Figure ~~&13~~ correspond to CS and
Figure ~~Fig.Figures~~ 10~~2~~ & ~~12~~
Figure 14 correspond to LB sand). Each figure contains three section planes (2D) at heights of 0 m (centre), 0.02 m, m and a 3D view at 0.06 m height to show temperature propagation in the HGHE system. The model results were compared with the experimental data at 8 hours after the start of charging and start of discharging. Temperatures extracted from the temperature distributions experimentally and numerically are summarised in ~~Tables 6~~
Table ~~Tables 7~~ and 8~~7~~ for charging and discharging respectively.

As evident from Fig. ~~Figures~~ 9~~11~~ ~~12~~
Figure 14, the temperature distributions were uniform. During the charging process, hot HTF enters the system at 343 and the backfill starts heating up steadily.
Figure ~~Fig.Figures~~ 11~~9 and 10~~2 illustrate the temperature distribution in CS and LB backfilled section respectively, heating (charging). For LB backfill (
Figure ~~Figure Fig.~~ 10~~2~~), the average surface temperature in the centre was 327 K, and at the top was 302 K, meaning heated up by 29 K in the centre and only 4 K at the top during an 8 hour period. Conversely, for the CS filled system (
Figure ~~Fig. Figure~~ 9~~11~~), the HGHE was overall hotter compared to LB after an 8 hour charging period. The centre of an average surface temperature of 340 K and the top was 334 K. Temperature differences between the middle and top for HGHE charging were calculated to be 25 K and 6 K for LB and CS respectively. In the discharging process, cold HTF (293 K) is passed through the inlet to the heat exchanging pipe system to extract the stored thermal energy (heat) from the backfill to the outlet, cooling down the system. Fig. 1~~1~~3~~Figures 11~~ ~~and 12~~and 14 illustrates the temperature hours from the start of discharging in CS and LB backfilled sections respectively.
Figure ~~Fig. Figure~~ 12~~4~~ shows the temperature distributions after 8 hours of discharging with LB backfill. The centre the coldest at 310 K with the majority showing as blue (cooler) areas and the top layer is the hottest at 340 K, illustrating that the LB sand filled system loses the heat quickly. The CS filled system (Fig. 13~~1Figure 11~~), however, during the same time period of 8 hours the centre of the HGHE had higher average surface temperatures of 335 K at

the centre and top of 341 K. Again, similar temperature differences were calculated between the middle and top, of 30 K and 6 K for LB and CS respectively, for discharging.

6.3   Comparing experimental and numerical results

Table 7

Table Table 8 summarises numerical and experimental calculated temperature differences between inlet and outlet which were ~40 K for CS and ~20 K for LB sand. This means the thermal capacity of the HGHE system can be doubled by using CS instead of LB sand. These results indicate that in order to increase the thermal performance of the HGHE section and obtain more hot water from the outlet to be used for space heating purposes, CS material would be a better material to use in HGHE systems because (1) CS heats up quicker than LB, (2) the heat in CS backfilled systems is propagated from the centre to the top quicker compared to LB and (3) the small temperature difference in CS for charging and discharging between the centre and top makes it an excellent material to use for HGHEs systems. CS being a waste material makes it an attractive choice compared to other materials to use as backfills in HGHEs.

The summary of average surface temperatures obtained numerically from Fig.Figures 911 12, Figure 14 and from experimental testing are presented in Tables 6 and 7 Table Tables 7

Table and 8 for HGHE charging and discharging processes. The difference in numerical and experimental results is K where experimental results were slightly higher compared to numerical results, this could be due to systematic errors or thermocouple tolerance reading level. This relatively low temperature difference indicates that the results are in agreement and validate each other.

7.   Conclusions

In this study, an experimental set-up and numerical model were used to analyze the thermal storage capacity of several proposed backfills to be used in HGHE system. The aim of this study was to compare the temperature distribution development in different backfill materials with respect to time. The selected materials used for backfill were all construction and industrial waste landfills materials (CD&E and C&I) including: sand, crushed basalt, broken brick, crushed concrete, metallic by-products including copper slag, aluminium slag, mill-scale, iron ores (fine and pellets). Utilising these low cost and sustainable waste materials means the waste material is being recycled which reduces the requirement for landfilling. Thermal testing, a thermodynamic and uncertainty analysis were also conducted and discussed. The main conclusions that can be drawn from the study are listed below:

- Initial thermal testing results showed that metallic materials including CS, AOAO, MS, IFO, IFN had better heat storage performance, with up to 77% improvement, compared to sand alone. IP, CON, TBR, BAC, BAF materials had similar performance to sand and TBW had lower performance.
- Particle size distribution (gradation) was also found to be a significant parameter in backfill selection. Medium sized particle sizes (1.18-2mm) performed 92% better compared to course and fine gradations of the same material.
- Various percentages of the backfill material (20, 40, 60, 80 and 100%) blended with remaining percentage of sand shows that the higher the percentage addition of the waste material the better the heat storage, by up to 77%.
- The data obtained from experimental and numerical analysis were in good agreement with each other.
- Designing the numerical model was important in determining the thermal operation and performance behavior of the HGHE storage and to ensure favorable conditions are satisfied prior to experimental testing.
- Both experimental and numerical model results were affected by the thermal-physical properties of the materials, including density and thermal conductivity.
- Results obtained from both experimental and numerical studies show the temperature range and duration of hot water produced from the system were in line with low temperature space heating guidelines and that mill-scale, copper slag and aluminium were the best backfill materials, where the thermal capacity of the HGHE system can be doubled using them compared to sand alone.

Abbreviations

GHEs	ground heat exchangers
HGHE	horizontal ground heat exchanger
GSHP	ground source heat pump
FVM	finite volume method
CFD	computational fluid dynamic
XEPS	extruded polystyrene foam insulation
HTF	heat transfer fluid
PSD	particle size distribution
FB	from bottom of HGHE (baseline)
MDF	modified density fibreboard
WMP	waste management plans
C&I	commercial & industrial waste
CD&E	construction, demolition and excavation waste
EC	environmental climatic chamber
LB	leighton buzzard sand
TBR	crushed brick – Type R
TBW	crushed brick – Type W
IP	iron ore pellets
IFN	fine iron ore powder – Type N
IFO	fine iron ore powder – Type O
AOAO	aluminum slag
CS	copper slag
MS	mill-scale
BAF	fine crushed basalt
BAC	course crushed basalt
CON	crushed concrete
UG	uniformly graded
CG	course graded
WG	well graded

Nomenclature

ρ	density of material (kg/m^3)
ρ_b	bulk density of material (kg/m^3)
ρ_s	particle density of material (kg/m^3)
C_p	specific heat capacity of material (J/kg K)
ϕn	porosity of material (%)
$k\,K$	thermal conductivity of material (W/mK)
γ_d	dry density of material (kg/m^3)
γ_s	solid density of material (kg/m^3)
T_{EC}	temperature inside environmental chamber (°C)
T_{AMB}	ambient room temperature (°C)
V_{HTF}	mean velocity of the HTF (m/s)
$\dot{m}_{HTF}$	mass flowrate of the HTF (kg/s)

ρ_{HTF}	density of the HTF (kg/m³)
A_{pipe}	cross-sectional area of the pipe (m²)
Re	calculated Reynolds number for the flow in the pipe
Q	volumetric flowrate (m³/s)
D_H	hydraulic diameter of the pipe (m)
h_c	convection heat transfer coefficient (W/m²K)
Nu	Nusselt number
k_{air}	thermal conductivity of air (W/mK)
L	distance from the pipe to the location of the top/bottom surface plane (m)
Pr	Prandtl number
Pe	Péclet number
U_x	free stream velocity (m/s)
v	kinematic viscosity of the HTF (m²/s)
μ	dynamic viscosity of the HTF (Ns/m²)
$C_{p_{HTF}}$	specific heat of the HTF (J/kgK)
k_{HTF}	thermal conductivity of the HTF (W/mK).
Q_{in}	energy required to raise the temperature of the backfill material in the HGHE (kJ)
m_{BF}	mass of backfill material in the HGHEs (kg)
$C_{p,BF}$	specific heat of the backfill material (KJ/kgK)
$T_{e,BF}$	temperature of backfill material at the end of the heating process (K)
$T_{s,BF}$	temperature of backfill material at the start of the heating process (K)
Q_{ext}	energy extracted from the HGHE using the HTF (kW~~J~~)
$\dot{m}_{HTF}$	mass flowrate of the HTF (kg/s)
Cp_{HTF}	specific heat of the HTF (k~~K~~J/kgK)
$T_{HTF,o}$	temperature of the HTF at the outlet of the HGHE system (K)
$T_{HTF,i}$	temperature of the HTF entering the HGHE system at the inlet (K)

References

Al-Ameen, Y., Ianakiev, A. and Evans, R. (2017) 'Thermal performance of a solar assisted horizontal ground heat exchanger', *Energy*. Elsevier Ltd, 140, pp. 1216–1227. doi: 10.1016/j.energy.2017.08.091.

Awani, S. *et al.* (2017) 'Numerical and experimental study of a closed loop for ground heat exchanger coupled with heat pump system and a solar collector for heating a glass greenhouse in north of Tunisia', *International Journal of Refrigeration*. Elsevier Ltd, 76, pp. 328–341. doi: 10.1016/j.ijrefrig.2017.01.030.

Axaopoulos, P. J. and Fylladitakis, E. D. (2013) 'Performance and economic evaluation of a hybrid photovoltaic/thermal solar system for residential applications', *Energy and Buildings*. Elsevier B.V., 65, pp. 488–496. doi: 10.1016/j.enbuild.2013.06.027.

Ball, D. A., Fischer, R. D. and Hodgett, D. L. (1983) 'Design methods for ground-source heat pumps', *ASHRAE Trans.*, 89, pp. 416–440. Bertermann, D., Klug, H. and Morper-busch, L. (2015) 'A pan-European planning basis for estimating the very shallow geothermal energy potentials', *Renewable Energy*. Elsevier Ltd, 75, pp. 335–347. doi: 10.1016/j.renene.2014.09.033.

Bourrelle, J. S., Andresen, I. and Gustavsen, A. (2013) 'Energy payback: An attributional and environmentally focused approach to energy balance in net zero energy buildings', *Energy and Buildings*. Elsevier B.V., 65, pp. 84–92. doi: 10.1016/j.enbuild.2013.05.038.

Chiasson, A. D. (2010) 'Modeling horizontal ground heat exchangers in geothermal heat pump systems', *COMSOL Conference 2010*. Available at: https://www.comsol.jp/paper/download/114861/chiasson_paper.pdf.

Congedo, P. M., Colangelo, G. and Starace, G. (2012) 'CFD simulations of horizontal ground heat exchangers : A comparison among different con fi gurations', *Applied Thermal Engineering*. Elsevier Ltd, 33–34, pp. 24–32. doi: 10.1016/j.applthermaleng.2011.09.005.

Cui, P., Yang, H. and Fang, Z. (2008) 'Numerical analysis and experimental validation of heat transfer in ground heat exchangers in alternative operation modes', *Energy and Buildings*, 40, pp. 1060–1066. doi: 10.1016/j.enbuild.2007.10.005.

DEFRA (2017) 'Digest of Waste and Resource Statistics – 2017 Edition', *Department for Environment Food & Rural Affairs*, (March). Available at: https://www.gov.uk/government/uploads/system/uploads/attachment_data/file/607416/Digest_of_Waste_and_Resource_Statistics__2017_rev.pdf .

Dehghan B., B. (2017) 'Experimental and computational investigation of the spiral ground heat exchangers for ground source heat pump applications', *Applied Thermal Engineering*. Elsevier Ltd, 121, pp. 908–921. doi: 10.1016/j.applthermaleng.2017.05.002.

Deloitte (2015) *Construction and Demolition Waste management in United Kingdom*.

Deru, M. (2003) *A Model for Ground-Coupled Heat and Moisture Transfer from Buildings A Model for Ground-Coupled Heat and Moisture Transfer from Buildings*.

Diaz, S. E., Sierra, J. M. T. and Herrera, J. A. (2013) 'The use of earth-air heat exchanger and fuzzy logic control can reduce energy consumption and environmental concerns even more', *Energy and Buildings*. Elsevier B.V., 65, pp. 458–463. doi: 10.1016/j.enbuild.2013.06.028.

Formatted: Normal, Left, Indent: Before: 0.5 cm

Dincer, I. and Rosen, M. a. (2004) 'Exergy as a Driver for Achieving Sustainability', *International Journal of Green Energy*, 1(1), pp. 1–19. doi: 10.1081/GE-120027881.

Emmi, G. *et al.* (2015) 'Solar assisted ground source heat pump in cold climates', *Energy Procedia*. Elsevier B.V., 82, pp. 623–629. doi: 10.1016/j.egypro.2015.12.010.

Esen, H., Esen, M. and Ozsolak, O. (2016) 'Modelling and experimental performance analysis of solar-assisted ground source heat pump system', *Experimental & Theoretical Artificial Intelligence*, (September 2015). doi: 10.1080/0952813X.2015.1056242.

Esen, H., Inalli, M. and Esen, Y. (2009) 'Temperature distributions in boreholes of a vertical ground-coupled heat pump system', *Renewable Energy*. Elsevier Ltd, 34(12), pp. 2672–2679. doi: 10.1016/j.renene.2009.04.032.

Esen, H. and Turgut, E. (2015) 'Optimization of operating parameters of a ground coupled heat pump system by Taguchi method', *Energy and Buildings*. Elsevier B.V., 107(November), pp. 329–334. doi: 10.1016/j.enbuild.2015.08.042.

Esen, M. (2000) 'Thermal performance of a solar-aided latent heat store used for space heating by heat pump', *Solar Energy*, 69(1), pp. 15–25. doi: 10.1016/S0038-092X(00)00015-3.

Esen, M. and Yuksel, T. (2013) 'Experimental evaluation of using various renewable energy sources for heating a greenhouse', *Energy and Buildings*. Elsevier B.V., 65, pp. 340–351. doi: 10.1016/j.enbuild.2013.06.018.

Farouki, O. T. (1986) 'Thermal Properties of Soils', *Series on Rock and Soil Mechanics*, 11, p. 136. doi: 10.1097/00010694-195008000-00030.

Florides, G. and Kalogirou, S. (2007) 'Ground heat exchangers-A review of systems, models and applications', *Renewable Energy*, 32(15), pp. 2461–2478. doi: 10.1016/j.renene.2006.12.014.

Gan, G., Riffat, S. B. and Chong, C. S. A. (2007) 'A novel rainwater – ground source heat pump – Measurement and simulation', *Applied Thermal Engineering*, 27, pp. 430–441. doi: 10.1016/j.applthermaleng.2006.07.011.

Gao, L. *et al.* (2013) 'Experimental study of a building-integrated solar air heating system in cold climate of China', *Energy and Buildings*. Elsevier B.V., 65, pp. 359–367. doi: 10.1016/j.enbuild.2013.06.014.

Garber, D., Choudhary, R. and Soga, K. (2013) 'Risk based lifetime costs assessment of a ground source heat pump (GSHP) system design: Methodology and case study', *Building and Environment*. Elsevier Ltd, 60, pp. 66–80. doi: 10.1016/j.buildenv.2012.11.011.

Garcia Gonzalez, R. *et al.* (2012) 'Interactions between the physical soil environment and a horizontal ground coupled heat pump, for a domestic site in the UK', *Renewable Energy*. Elsevier Ltd, 44, pp. 141–153. doi: 10.1016/j.renene.2012.01.080.

Go, G. H. *et al.* (2015) 'A new performance evaluation algorithm for horizontal GCHPs (ground coupled heat pump systems) that considers rainfall infiltration', *Energy*. Elsevier Ltd, 83, pp. 766–777. doi: 10.1016/j.energy.2015.02.086.

Henning, H. M. (2007) 'Solar assisted air conditioning of buildings - an overview', *Applied Thermal Engineering*, 27(10), pp. 1734–1749. doi: 10.1016/j.applthermaleng.2006.07.021.

Hepbasli, A., Akdemir, O. and Hancioglu, E. (2003) 'Experimental study of a closed loop vertical ground source heat pump system', *Energy Conversion and Management*, 44(4), pp. 527–548. doi: 10.1016/S0196-8904(02)00073-0.

Holman, J. P. (1994) *Experimental Methods for Engineers*. sixth ed. Singapore: McGraw-Hill.

Hu, P. *et al.* (2013) 'Performance study of a ground heat exchanger based on the multipole theory heat transfer model', *Energy and Buildings*. Elsevier B.V., 65, pp. 231–241. doi: 10.1016/j.enbuild.2013.06.002.

Inalli, M. and Esen, H. (2004) 'Experimental thermal performance evaluation of a horizontal ground-source heat pump system', *Applied Thermal Engineering*, 24(14–15), pp. 2219–2232. doi: 10.1016/j.applthermaleng.2004.01.005.

İnallı, M. and Esen, H. (2004) 'Experimental thermal performance evaluation of a horizontal ground-source heat Engineering, Applied Thermalpump system', *Applied Thermal Engineering*, 2219–2232. doi: 10.1016/j.applthermaleng.2004.01.005.

Kim, M.-J. *et al.* (2016a) 'Thermal performance evaluation and parametric study of a horizontal ground heat exchanger', *Geothermics*. CNR-Istituto di Geoscienze e Georisorse, 60, pp. 134–143. doi: 10.1016/j.geothermics.2015.12.009.

Kim, M.-J. *et al.* (2016b) 'Thermal performance evaluation and parametric study of a horizontal ground heat exchanger', *Geothermics*. CNR-Istituto di Geoscienze e Georisorse, 60(January), pp. 134–143. doi: 10.1016/j.geothermics.2015.12.009.

Koyun, A., Demir, H. and Torun, Z. (2009) 'Experimental study of heat transfer of buried finned pipe for ground source heat pump applications', *International Communications in Heat and Mass Transfer*. Elsevier Ltd, 36(7), pp. 739–743. doi: 10.1016/j.icheatmasstransfer.2009.03.022.

Kupiec, K., Larwa, B. and Gwadera, M. (2015) 'Heat transfer in horizontal ground heat exchangers', *Applied Thermal Engineering*. Elsevier Ltd, 75, pp. 270–276. doi: 10.1016/j.applthermaleng.2014.10.003.

Leong, W. ., Tarnawski, V. . and Aittomäki, A. (1998) 'Effect of soil type and moisture content on ground heat pump performance', *International Journal of Refrigeration*, 21(8), pp. 595–606. doi: 10.1016/S0140-7007(98)00041-3.

Li, X. *et al.* (2006) 'Thermal performances of different types of underground heat exchangers', *Energy and Buildings*, 38(5), pp. 543–547. doi:

10.1016/j.enbuild.2005.09.002.

Lund, H. (2010) 'European long-term trends in recycled gypsum usage Perfect Bagging', *global gypsum magazine*, (November), pp. 24–28.

Lund, H. *et al.* (2016) 'Energy Storage and Smart Energy Systems', *International Journal of Sustainable Energy Planning and Management*, 11, pp. 3–14. doi: 10.5278/ijsepm.2016.11.2.

Luo, J. *et al.* (2016) 'A review of ground investigations for ground source heat pump (GSHP) systems', *Energy and Buildings*. Elsevier B.V., 117, pp. 160–175. doi: 10.1016/j.enbuild.2016.02.038.

Naylor, S., Ellett, K. M. and Gustin, A. R. (2015) 'Spatiotemporal variability of ground thermal properties in glacial sediments and implications for horizontal ground heat exchanger design', *Renewable Energy*. Elsevier Ltd, 81, pp. 21–30. doi: 10.1016/j.renene.2015.03.006.

Ozgener, O. and Hepbasli, A. (2005) 'Experimental performance analysis of a solar assisted ground-source heat pump greenhouse heating system', *Energy and Buildings*, 37(1), pp. 101–110. doi: 10.1016/j.enbuild.2004.06.003.

Ozyurt, O. and Ekinci, D. A. (2011) 'Experimental study of vertical ground-source heat pump performance evaluation for cold climate in Turkey', *Applied Energy*. Elsevier Ltd, 88(4), pp. 1257–1265. doi: 10.1016/j.apenergy.2010.10.046.

Qoaider, L., Kiwan, S. and Thabit, Q. (2016) 'Investigation of the Flowability and the Thermal Behavior of Sand / Basalt-Mixture in Moving Bed Heat Exchanger (MBHX) as Heat Transfer Medium for Concentrating Solar Tower Plants', 10(4), pp. 263–270.

Rees, S. J. (2016) *Horizontal and compact ground heat exchangers, Advances in Ground-Source Heat Pump Systems*. Elsevier Ltd. doi: 10.1016/B978-0-08-100311-4.00005-4.

Rees, S. W. *et al.* (2000) 'Ground heat transfer effects on the thermal performance of earth-contact structures', *Renewable & sustainable energy reviews*, 4(3), pp. 213–265. doi: 10.1016/S1364-0321(99)00018-0.

Sarbu, I. and Sebarchievici, C. (2014) 'General review of ground-source heat pump systems for heating and cooling of buildings', *Energy and Buildings*. Elsevier B.V., 70(February 2014), pp. 441–454. doi: 10.1016/j.enbuild.2013.11.068.

Shang, Y., Dong, M. and Li, S. (2014) 'Intermittent experimental study of a vertical ground source heat pump system', *Applied Energy*. Elsevier Ltd, 136, pp. 628–635. doi: 10.1016/j.apenergy.2014.09.072.

Simms, R. B., Haslam, S. R. and Craig, J. R. (2014) 'Impact of soil heterogeneity on the functioning of horizontal ground heat exchangers', *Geothermics*. CNR-Istituto di Geoscienze e Georisorse, 50, pp. 35–43. doi: 10.1016/j.geothermics.2013.08.007.

Sivasakthivel, T., Murugesan, K. and Thomas, H. R. (2014) 'Optimization of operating parameters of ground source heat pump system for space heating and cooling by Taguchi method and utility concept', *Applied Energy*. Elsevier Ltd, 116(February), pp. 76–85. doi: 10.1016/j.apenergy.2013.10.065.

Stylianou, I. I. *et al.* (2017) 'Methodology for estimating the ground heat absorption rate of Ground Heat Exchangers', *Energy*, 127, pp. 258–270. doi: 10.1016/j.energy.2017.03.070.

Tarnawski, V. R. *et al.* (2009) 'Analysis of ground source heat pumps with horizontal ground heat exchangers for northern Japan', *Renewable Energy*, 34(1), pp. 127–134. doi: 10.1016/j.renene.2008.03.026.

Wei, K. *et al.* (2017) 'Study on a design method for hybrid ground heat exchangers of ground-coupled heat pump system', *International Journal of Refrigeration*. Elsevier Ltd, 76, pp. 394–405. doi: 10.1016/j.ijrefrig.2016.12.020.

Wong B., Snijders A., M. L. (2006) 'Recent Inter-seasonal Underground Thermal Energy Storage Applications in Canada', *IEEE EIC Climate Change Technology*, pp. 1–7.

WRAP, W. resource action programme. (2010) *Environmental benefits of recycling - 2010 update, Environmental benefits of recycling - 2010 update*. Available at: http://www.wrap.org.uk/sites/files/wrap/Environmental_benefits_of_recycling_2010_update.3b174d59.8816.pdf.

Wu, Y. *et al.* (2010) 'Experimental measurement and numerical simulation of horizontal-coupled slinky ground source heat exchangers', *Applied Thermal Engineering*. Elsevier Ltd, 30(16), pp. 2574–2583. doi: 10.1016/j.applthermaleng.2010.07.008.

Wu, Y. *et al.* (2011) 'Prediction of the thermal performance of horizontal-coupled ground-source heat exchangers', *International Journal of Low Carbon Technologies*, (July), pp. 261–269. doi: 10.1093/ijlct/ctr013.

Yoon, S., Lee, S.-R. and Go, G.-H. (2015) 'Evaluation of thermal efficiency in different types of horizontal ground heat exchangers', *Energy and Buildings*. Elsevier B.V., 105, pp. 100–105. doi: 10.1016/j.enbuild.2015.07.054.

Table 1. ÷Experimental HGHE system technical information

Location: Nottingham, UK (Lat. 52°57'26"N, -Long. 1°9'8"W)	
Heating load of design test room	
Dimensions (m)	5L x 3W x 3H
Concrete floor/ceiling plan area (m^2)	15
Volume of room (m^3)	45
Heating load requirement (kW)	1
Comfort room temperature (℃)	20
Window area (m^2)	2
Brick wall area (m^2)	39
Ground heat exchanger information	
Type	Horizontal Loop
Pipe material	Copper
Total length of pipe (m)	15
Each layer length of pipe (m)	5
Pipe external diameter (m)	0.01
Pipe internal diameter (m)	0.007
Pipe loop spacing (m)	0.085
Heat transfer fluid type	Water
Cold water inlet temperature (℃)	20
Hot water outlet temperature (℃)	70
GSHP used	None
Insulation used (See Error! Reference source not found.Table 2)	Yes
	Yes
Containment used (See Error! Reference source not found.Table 2)	

Table 2. Thermophysical properties of materials used in this study

Material and Abbreviation	Particle Size (mm)	Thickness (m)/ Gradation Classification	ρ_b (kg/m^3)	ρ_s (kg/m^3)	nϕ (%)	k (W/mK)	Cp (J/kg K)

15

HGHE construction materials:

Cover (MDF)	-	0.025m	700	-	-	0.15	1700
Insulation (XEPS)	-	0.05m	33	-	-	0.03	1131
Copper Pipe	-	0.003m	8950	-	-	401	385
Water liquid (HTF)	-		1000	-	-	0.60	4200
Air (external environment)	-		1.23	-	-	0.02	1006

HGHE backfill materials:

Leighton Buzzard Sand (LB)	0.16 – 1.18	UG	1562.49	2620.80	40.40	0.38	805.87
Crushed Brick 'W type' (TBW)	0.06 – 5.00	WG	1142.46	2631.37	56.60	0.65	860.02
Crushed Brick 'R type' (TBR)	0.16 – 5.00	WG	974.45	2275.70	57.20	0.62	834.45
Concrete (CON)	0.16 – 14.00	WG	1204.07	2280.30	47.20	1.28	645.33
Basalt rock 'fine' (BAF)	0.16 – 5.00	GG	1496.53	2681.00	44.20	2.04	884.35
Basalt rock 'course' (BAC)	6.30 – 10.00	UG	2389.61	2704.45	49.32	1.24	907.21
Iron ore pellets (IP)	10.00 – 14.00	CG	2080.42	3954.37	47.40	0.56	616.50
Iron Fillings 'N type' (IFN)	0.16 – 3.35	WG	2596.82	3728.91	30.38	0.60	580.07
Iron Filings 'O type' (IFO)	0.16 – 3.35	WG	3250.51	3668.17	11.40	0.55	546.14
Millscale (MS)	0.16 – 6.30	UG	2544.48	3133.00	18.80	0.42	652.39
Copper slag (CS)	0.43 – 2.00	UG	1992.03	3399.32	41.40	0.78	557.21
Aluminium slag (AO)	0.60 – 2.00	UG	1897.96	3641.36	47.90	17.34	476.75

Table 3. Boundary conditions used in the HGHE numerical model

Region	Boundary condition type	Condition	Thermal Boundary (charging mode) Temperature (K)	Thermal Boundary (discharging mode) Temperature (K)
Inlet	Velocity Inlet	0.3m/s	343.15	293.15
Outlet	Pressure Outlet	0 Pressure	343.15	293.15
Wall Insulation	Convection		293.15	343.15
Wall Cover	Convection		293.15	343.15
Wall Soil	Convection		293.15	343.15

Table 4. Summary of Q_{in} calculated for the HGHEs with each of the backfill materials

Material used as backfill	Q_{in} (kJ)
LB	3934.89
TBW	3070.43
TBR	2541.03
CON	2428.19
BAF	4135.80
BAC	5425.06
IP	4008.06
IFN	4707.30
IFO	5547.60
MS	5187.48
CS	5919.17
AO	6774.62

Note: The Q_{in} values in Table 4 were calculated using equation 7. The calculations used a temperature difference of 50K where: $T_{startBF}$ and T_{inwa} are assumed to be 293K and; T_{endBF} and T_{outwa} are assumed to be 343K.

Table 5. The experimental results and total uncertainties of the measured parameters

Item	Average Value	Total uncertainty (%)
HTF temperature at HGHE inlet ($T_{HTF,i}$)	21 °C	± 1.38
HTF temperature at HGHE outlet ($T_{HTF,O}$)	70 °C	± 1.38
Ambient room temperature (T_{AMB})	16 °C	± 1.38
Average temperature at top and bottom of backfill material	20 °C	± 1.38
Mass flowrate of HTF ($\dot{m}_{HTF}$)	0.0016 – 0.01 kg/s	± 2.89

Table 6. Results for Re, Pe, Nu and hc

S. No	$\dot{m}_{HTF}$ (kg/s)	$\vec{V}_{HTF}$ (m/s)	Re_x	Pe	Nu (theoretical)	Nu (numerical)	hc (kW/m²K)
1	0.0017	0.0441	474.96	2044.64	23.54	20.84	2.13
2	0.0034	0.0883	949.97	4089.28	33.29	30.09	3.01
3	0.0068	0.1767	1899.94	8178.56	47.08	43.68	4.25
4	0.0120	0.3118	3352.84	14432.75	62.54	59.41	5.65

Note: Pr = 4.30

Table 7. Comparison of experimental and numerical results when charging HGHE model at time = 8 hours (8 hours from start of process)

Material	Experimental or Numerical (E or N)	Average surface temperature at 0m from middle (K)	Average surface temperature at 0.04m from middle (K)	Average surface temperature at 0.06m from middle (K)	Temperature difference between centre and top surface (K)
LB	E	329	312	306	23
LB (Fig. 12)	N	327	309	302	25
CS	E	342	339	332	10
CS (Fig. 11)	N	340	336	334	6

Note: The numbers mentioned in Table 7 were recorded at 8 hours after charging where: Backfill start = 293 K, Inlet = 343 K

Table 8. Comparison of experimental and numerical results when discharging HGHE model at time = 8 hours (8 hours from start of discharging process)

Material	Experimental or Numerical (E or N)	Average surface temperature at 0m from middle (K)	Average surface temperature at 0.04m from middle (K)	Average surface temperature at 0.06m from middle (K)	Temperature difference between centre and top surface (K)	Temperature difference between the inlet (293K) and outlet of HTF (K)
CS	E	331	342	345	4	39
CS (Fig. 13)	N	335	339	341	6	42
LB	E	315	329	344	29	23
LB (Fig. 14)	N	310	327	340	30	19

Note: The numbers mentioned in Table 8 were recorded at 8 hours after discharging where: Backfill start = 343 K, Inlet = 293 K
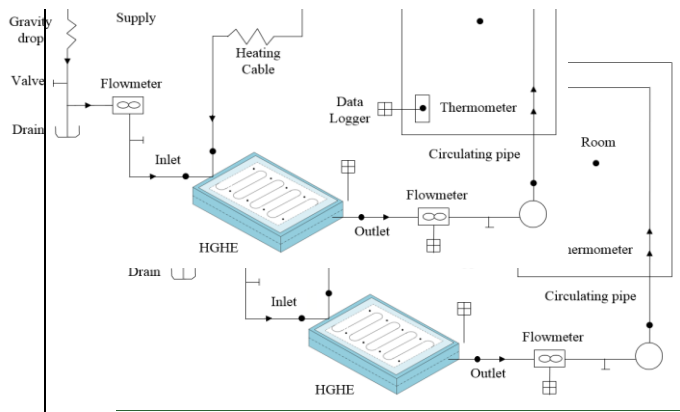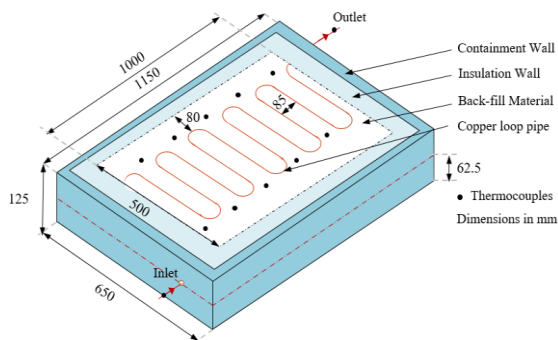
Figure 1. ÷Schematic diagram of the HGHE system

Figure 2. ÷3D schematic diagram of the HGHE set-up storage used in the experimental and numerical model

Figure 3. ÷Materials utilised in this study; Rows from left to right: Top: LB, TBR, TBW, IP.
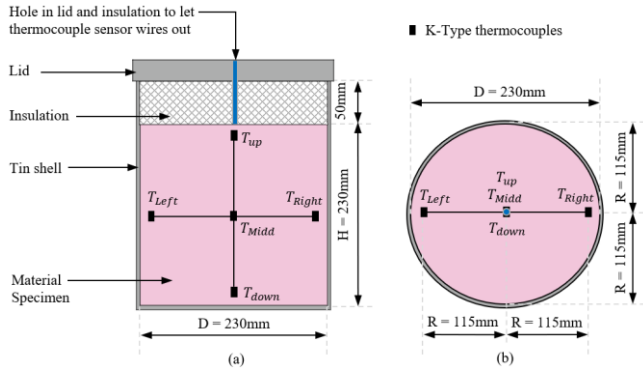Middle: IFN, IFO, AOÐ, CS. Bottom: MS, BAF, BAC, CON.

Figure 4. Cross sectional schematic diagram of the containers used for testing (Dimensions in mm)
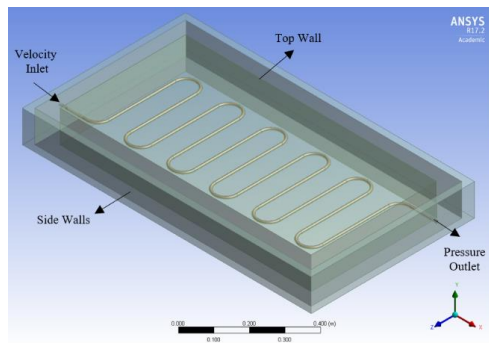
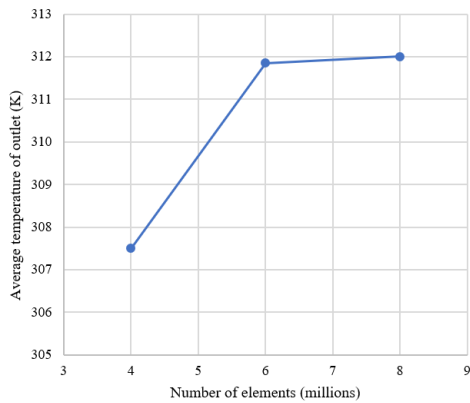Figure 45. ÷Velocity inlets, pressure outlet and wall specified on the numerical model in ANSYS Fluent

Figure 6. Mesh independence study evaluation
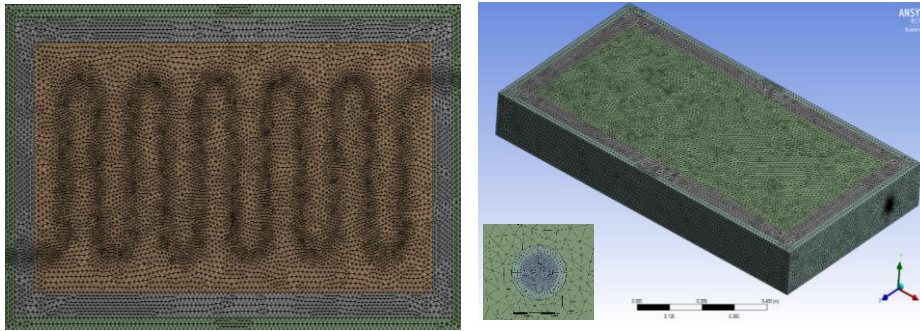
Figure 7. The meshed HGHE model. Right: 3D mesh with pipe detail. Left: Cross section through centre of HGHE
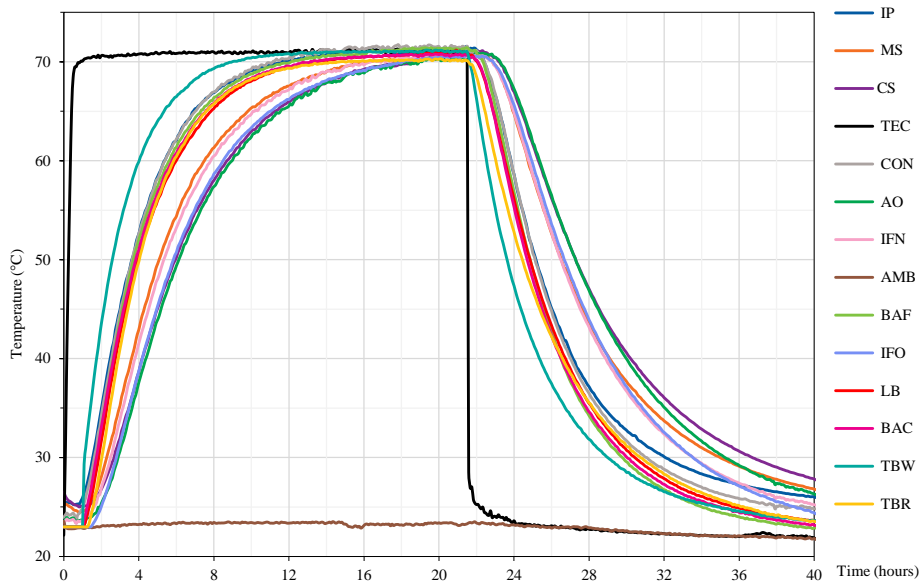
Formatted: Font color: Blue

Figure 8. ÷Temperature vs. time thermal test results using various backfill material's as heat storage medias
Note: where TEC is the internal temperature measured in the climatic chamber, AMB is the recorded ambient testing room temperature
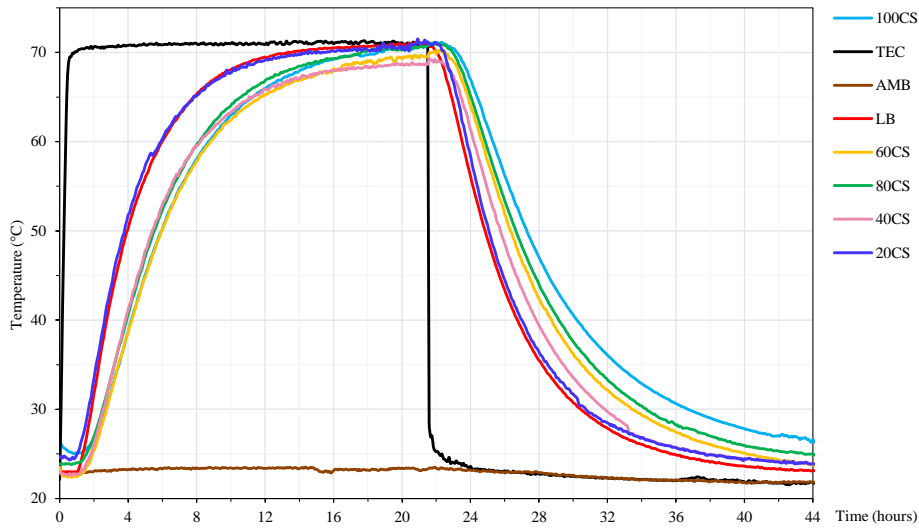

Figure 9. ÷Temperature vs. time thermal test results using different percentages of CS material with LB sand
Note: 100CS (100% CS), 80CS (80% CS and 20% LB Sand), 60CS (60% CS and 40% LB Sand), 40CS (40% CS and 60% LB Sand), 20 CS (20% CS and 80% LB Sand) and LB (100% LB Sand).
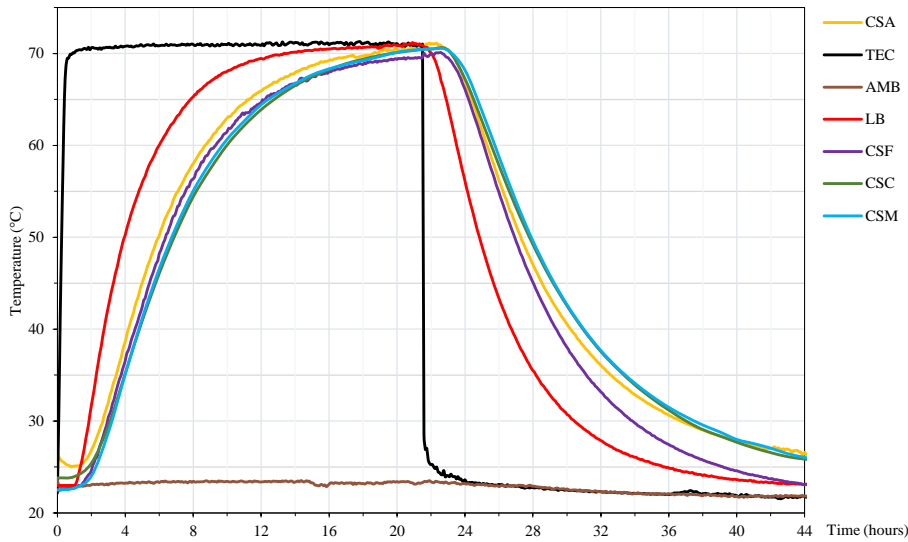
Figure 10. ÷Temperature vs. time thermal test results using different particle size gradations of CS material
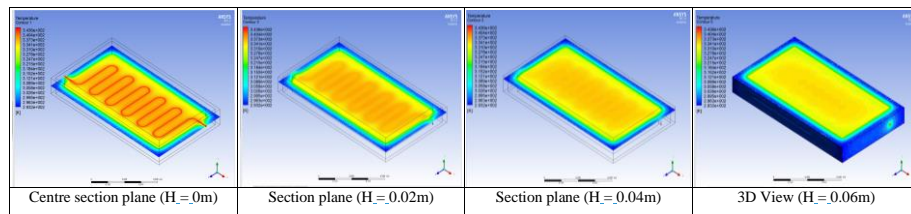Note: CSA (0.43 - 2mm), CSF (<0.6mm), CSM (0.6-1.18mm), CSC (1.18-2mm)

| Centre section plane (H =0m) | Section plane (H =0.02m) | Section plane (H =0.04m) | 3D View (H =0.06m) |

Figure 11. ÷Temperature distributions of HGHE backfilled with CS material after 8 hours from start of charging

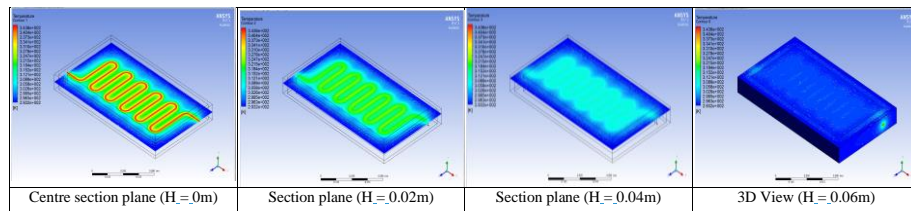| Centre section plane (H =0m) | Section plane (H =0.02m) | Section plane (H =0.04m) | 3D View (H =0.06m) |

Figure 12. ÷Temperature distributions of HGHE backfilled with LB sand material after 8 hours from start of charging
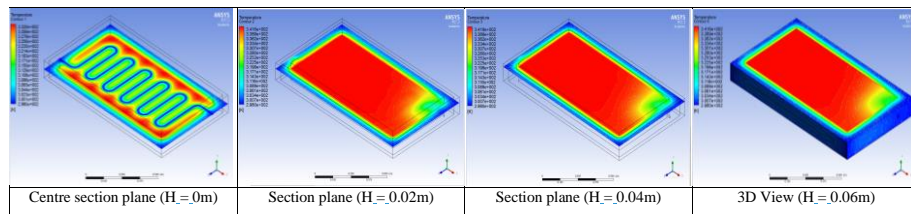
Formatted: Indent: Before: 0 cm

22

Centre section plane (H = 0m)	Section plane (H = 0.02m)	Section plane (H = 0.04m)	3D View (H = 0.06m)

Figure 13. Temperature distributions of HGHE backfilled with CS material after 8 hours from start of discharging

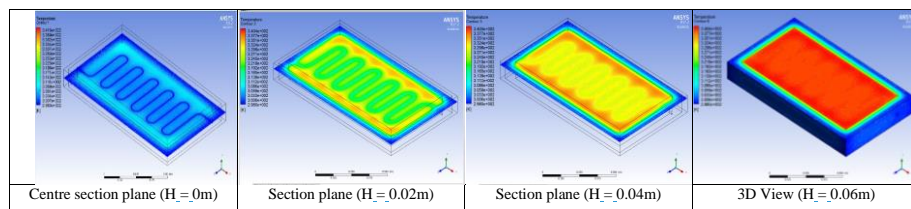| Centre section plane (H = 0m)	Section plane (H = 0.02m)	Section plane (H = 0.04m)	3D View (H = 0.06m)

Figure 14. Temperature distributions of HGHE backfilled with LB material after 8 hours from start of discharging

Formatted: Indent: Before: 0 cm

23